INTERNATIONAL JOURNAL OF HYDROGEN ENERGY 35 (2010) 6634–6645

Available at www.sciencedirect.com

ScienceDirect

journal homepage: www.elsevier.com/locate/he

Steady-state and dynamic modeling of biohydrogen production in an integrated biohydrogen reactor clarifier system

Hisham Hafez [a], *M. Hesham El. Naggar* [a,*], *George Nakhla* [a,b]

[a] *Department of Civil Engineering, The University of Western Ontario, London, Ontario N6A 5B9, Canada*
[b] *Department of Chemical and Biochemical Engineering, The University of Western Ontario, London, Ontario N6A 5B9, Canada*

ARTICLE INFO

Article history:
Received 1 March 2010
Received in revised form
29 March 2010
Accepted 2 April 2010
Available online 21 May 2010

Keywords:
Biological hydrogen production
Steady-state modeling
Dynamic modeling
IBRCS

ABSTRACT

Steady-state operational data from the integrated biohydrogen reactor clarifier system (IBRCS) during anaerobic treatment of glucose-based synthetic wastewater at HRT of 8 h and SRT ranging from 26 to 50 h and organic loading rates of 6.5–206 gCOD/L-d were used to calibrate and verify a process model of the system developed using BioWin. The model accurately predicted biomass concentrations in both the bioreactor and the clarifier supernatant with average percentage errors (APEs) of 4.6% and 10%, respectively. Hydrogen production rates and hydrogen yields predicted by the model were in close agreement with the observed experimental results as reflected by an APE of less than 4%, while the hydrogen content was well correlated with an APE of 10%. The successful modeling culminated in the accurate prediction of soluble metabolites, i.e. volatile fatty acids in the reactor with an APE of 14%. The calibrated model confirmed the advantages of decoupling of the solids retention time (SRT) from the hydraulic retention time (HRT) in biohydrogen production, with the average hydrogen yield decreasing from 3.0 mol H_2/mol glucose to 0.8 mol H_2/mol glucose upon elimination of the clarifier. Dynamic modeling showed that the system responds favorably to short-term hydraulic and organic surges, recovering back to the original condition. Furthermore, the dynamic simulation revealed that with a prolonged startup periods of 10 and 30 days, the IBRCS can be operated at an HRT of 4 h and OLR as high as 206 gCOD/L-d without inhibition and/or marked performance deterioration.
© 2010 Professor T. Nejat Veziroglu. Published by Elsevier Ltd. All rights reserved.

1. Introduction

Biological hydrogen production from renewable sources (biomass, water, and organic wastes) [1] has the potential to meet the growing demand for energy. It offers a feasible means for sustainable supply of H_2 with low pollution and high efficiency, thereby considered a promising eco-friendly energy source [2]. Comparing the production rates of H_2 by various biohydrogen systems and the associated operational complexity, suggest that dark-fermentation systems offer an excellent potential for practical applications. Although fermentative biohydrogen technologies are still in their infancy, the sustained efforts for developing more efficient technologies will eventually lead to economically feasible technologies. An important step to achieve these feasible solutions includes the development of a process model in order to perform process sensitivity analysis to facilitate the scale-up of the process.

* *Corresponding author*. Tel.: +1 519 661 4219; fax: +1 519 661 3942.
E-mail address: helnaggar@eng.uwo.ca (M.H.El. Naggar).
0360-3199/$ – see front matter © 2010 Professor T. Nejat Veziroglu. Published by Elsevier Ltd. All rights reserved.
doi:10.1016/j.ijhydene.2010.04.012

Hafez et al. [3] developed a novel integrated biohydrogen reactor clarifier system (IBRCS) [4] (see Fig. 1). The system is comprised of a continuously stirred reactor (CSTR) for biological hydrogen production, followed by an uncovered gravity settler for decoupling of solids retention time (SRT) from hydraulic retention time (HRT). The system was able to maintain a maximum hydrogen yield and production rate of 3.1 mol H_2/mol glucose and 191 L/d, respectively. The performance of the IBRCS underscores its potential as an efficient technology that is economically feasible for biological hydrogen production from organic wastes. However, a process model is necessary for better understanding the process and optimization of the system parameters.

Most studies on biohydrogen production modeling were performed considering batch systems using the Gompertz and Monod equations [5,6]. The Gompertz equation is an empirical formula where three model parameters (i.e. lag time, H_2 production potential, and H_2 production rate) are adjusted to fit the Gompertz equation to experimental hydrogen evolution data. Even though this curve-fitting approach yields high correlation coefficients between the observed and fitted hydrogen evolution data, the three model parameters determined by curve-fitting are restricted to specific experimental conditions and cannot be used in a predictive mode [5]. Due to its empirical nature, the utility of the Gompertz equation is severely limited as it cannot account for relevant process variables such as substrate concentrations, temperature, pH, substrate types, etc. In some studies, the Gompertz equation has been modified to accommodate typical kinetics of substrate degradation, biomass growth, and hydrogen production [7–9]. Some biohydrogen studies have utilized the conventional kinetic expressions such as Monod's equation [6–8,10,11]. However, rigorous and multiple simulations, followed by a series of validations may be required to establish the generality of such equations and the associated parameters. Furthermore, comprehensiveness of such models is accomplished only when they can be readily integrated with other complex bioprocesses, i.e. hydrolysis, acidogenesis, and H_2 production from complex and particulate organic substrates [5].

Whang et al. [12] developed a kinetic-based dual-substrate steady-state model using experimental data from a 2.5 L CSTR with a working volume of 1.5 L. The feedstock included 12,000 mg/L of glucose and 8000 mg/L of peptone. This model accurately predicted the biomass concentration since biomass growth depends mainly on glucose and nitrogen concentrations. By using complementary substrate and growth-associated product assumption, the model captured the general trends of consumption of substrates and accumulation of products at dilution rate (D) conditions between 0.06 and 0.69/h. The model predicted that an increase in D from 0.06 to 0.5/h minimized the adverse effects of endogenous respiration and peptone metabolism on net hydrogen production, leading to an increase in hydrogen production rate from 58.6 to 1478 mmol/L/day. For operational conditions of $D > 0.69$/h, washout of hydrogen-producing bacteria in the CSTR became substantial and resulted in a rapid drop in hydrogen production rate. The aforementioned authors observed that at the operational conditions approaching the critical minimum D of 0.69/h, the model overestimated the hydrogen production rate due to its overestimation of butyrate concentration and underestimation of formate concentration.

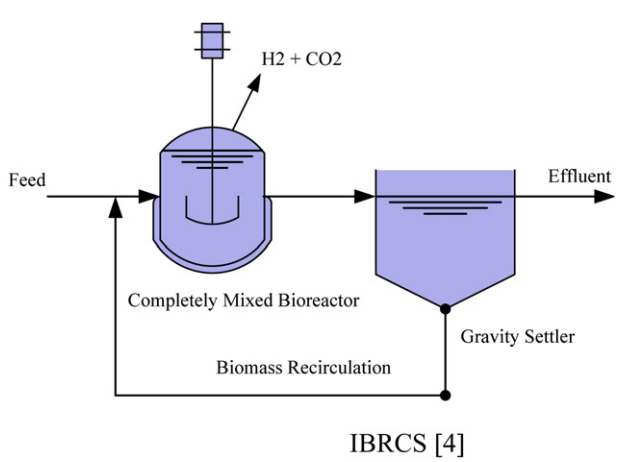

Fig. 1 – Experimental setup for the integrated biohydrogen reactor clarifier system.

Early mechanistic mathematical models of anaerobic digestion considered only methanogenic reactions based on the assumption that methane production is the rate limiting step in the process [13,14]. An initial extension of this conceptual framework included the reactions of "acid-formers" which considered both particulate hydrolysis and production of volatile fatty acids (VFAs) [15]. These early models represented the VFA concentration as one "bulk" component that was considered to be the sole substrate for the methanogens. The role of hydrogen in the regulation of product distribution and consumption was a key development that formed the basis for many subsequent models of anaerobic digestion [16]. This advancement allowed models to predict the formation of various fermentation products in addition to acetic acid, such as the higher acids propionic and butyric. In addition, methane production from both acetic acid and hydrogen could be included. A number of models were developed based on the "four population" framework of Mosey [16], including Costello et al. [17] and Jones et al. [18].

The Anaerobic Digestion Model I (ADM1) is a mechanistic model that has open structure and common nomenclature integrating: biokinetics with association–dissociation; gas–liquid transfer; and cellular processes involving hydrolysis, acidogenesis, acetogenesis, and methanogenesis. Previous researchers have successfully used the ADM1 model for describing methane production from mixed culture fermentation of domestic, industrial wastewater as well as solid wastes [19]. Peiris et al. [20] demonstrated the utility of ADM1 model in biohydrogen studies by simulating the effect of carbohydrate–protein ratio on dynamic production of protons, biomass, fatty acid and hydrogen. However, the curve-fitting of the experimental data was not sufficiently accurate for both the biohydrogen production and the intermediates concentrations in the liquid phase. The aforementioned authors modified the ADM1 model by including lactate and ethanol (two intermediate products in anaerobic digestion processes, excluded from the ADM1 model due to their low impact on methanogenic and low loaded systems) by the addition of four extra state variables; two for soluble lactate and ethanol and two for lactate-degrading and ethanol-

degrading organisms. The modified ADM predicted bioreactor pH well but failed to predict the hydrogen yield accurately, with errors well above 100% at carbohydrates-to-protein ratios of 1:4 and 0:5. Furthermore the model predicted biomass yield deviated significantly from the experimental data at carbohydrates-to-protein ratios of 2:3, 1:4 and 0:5.

Rodriguez et al. [21,22] recast the ADM1 model calculations in terms of mol/L (instead of gCOD/L) and predicted product formation by maximizing the biomass growth under different environmental conditions based on thermodynamic feasibility using variable biomass yields in steady-state modeling. However, under dynamic conditions, both constant and variable stoichiometric biomass yields achieved same results.

This comprehensive literature review demonstrates that no models are readily available that can accurately predict continuous biohydrogen production. On the other hand, most of the available anaerobic digestion models were derived for anaerobic digestion of municipal wastewater biosolids, which employ CSTR and are not capable of modeling a system that decouples the SRT from the HRT (a key feature of the IBRCS). One such model is incorporated in the software BioWin (EnviroSim Associates Ltd., Flamborough, Ontario, Canada), which is widely used for modeling wastewater treatment plants. However, it was never used for modeling biohydrogen production systems. Thus, the three objectives of this paper are: exploring the use of BioWin model for simulation of biohydrogen production in IBRCS using data from an experimental study [3], evaluating the beneficial effects of decoupling SRT from HRT by comparing the performance of the IBRCS with the conventional CSTR, and assessing the impact of short- and long-term hydraulic and organic loading rates using both steady-state and dynamic simulation along with the impact of startup hydraulic and organic loading rate on the performance of the IBRCS.

2. Materials and methods

This section provides a brief description of the experimental setup, procedures and operational used in collecting the experimental data for the IBRCS that is later used in the numerical models. Additional information can be found in Hafez et al. [3].

2.1. Systems setup and operations

Two lab-scale IBRCSs were considered in the study, each comprising a continuously stirred reactor (CSTR) for biological hydrogen production (5 L working volume), followed by an uncovered gravity settler (volume 8 L), i.e. open to the atmosphere for the decoupling of solids retention time (SRT) from the hydraulic retention time (HRT). Both systems were operated at 37° C for 220 days (Fig. 1), at six different organic loading rates (OLRs) ranging from 6.5 to 206 gCOD/L-d. Details of the operational conditions for the six runs are listed in Table 1. It is noteworthy that the systems were run at steady-state conditions for at least 20 turnovers of the mean SRT, with the shortest run lasting for 45 days and the longest run for 75 days, excluding the first week of startup. In order to enrich hydrogen-producing bacteria, the seed sludges were heat treated at 70° C for 30 min prior to startup. Following the completion of each run and the attainment of steady-state conditions, the systems were cleaned and inoculated with pre-treated sludges. OLR-1 and OLR-2 were run simultaneously, followed by OLR-3 and OLR-4, and lastly OLR-5 and OLR-6. The systems were monitored for total chemical oxygen demand (TCOD), soluble COD, volatile fatty acids (VFAs), ethanol, lactate, glucose, volatile suspended solids (VSS), total suspended solids (TSS) and biogas composition including hydrogen, methane and nitrogen. The quantity of produced biogas was recorded daily using a wet-tip gas meter (Rebel Wet-tip Gas Meter Company, Nashville, TN, USA). Details of analytical methods are reported elsewhere [3].

Table 1 – Operational conditions.

	Glucose (g/L)	HRT (h)	SRT (h)	OLR (gCOD/L-d)	Final pH
OLR-1	2	8	50 ± 5	6.5	5.5
OLR-2	8	8	45 ± 4	25.7	5.5
OLR-3	16	8	45 ± 6	51.4	5.5
OLR-4	32	8	42 ± 6	103	5.5
OLR-5	48	8	27 ± 3	154	5.5
OLR-6	64	8	26 ± 2	206	5.5

Note. Values represent average ± standard deviation.

2.2. Inocula and media compositions

Anaerobically digested sludge from the St. Marys wastewater treatment plant (St. Marys, Ontario, Canada) was used as the seed. The two systems operated in parallel at the same time under two different OLRs for a total of six OLRs (three consecutive runs). The systems were seeded with 5 L of sludge and started up in a continuous mode with the feed containing glucose at different concentrations as presented in Table 1. The same startup technique was repeated for the three runs. It must be emphasized that there was no sludge wastage from the clarifier throughout the operation, and the values of SRTs presented in Table 1 represent the average ± standard deviation (SD) during steady-state operation. It is noteworthy that the reactors operation was consistent over time and accordingly, the average SRT with SD of less than 10% of the mean SRT is representative of the overall SRT during the run.

As expected, the clarifier effluent VSS concentrations were substantially lower than the reactor VSS concentrations and remained unchanged during steady-state operation. The feed contained sufficient inorganics (mg/L): $NaHCO_3$, 2000–16,000; $CaCl_2$, 140; $MgCl_2 \cdot 6H_2O$, 160; NH_4HCO_3, 600; $MgSO_4 \cdot 7H_2O$, 160; urea, 500–2000; Na_2CO_3, 124–300; $KHCO_3$, 156; K_2HPO_4, 15–20; trace mineral solution, 500; H_3PO_4, 250–1500. Despite the lack of real-time pH control, buffering capacity was sufficient to maintain a final pH of 5.5 in all runs.

2.3. Model formulation

The anaerobic degradation processes in the BioWin model are based on the "four population" model concept (heterotrophs, acetogens, acetoclastic methanogenesis and hydrogenotrophic methanogenesis). To simulate the inhibition of

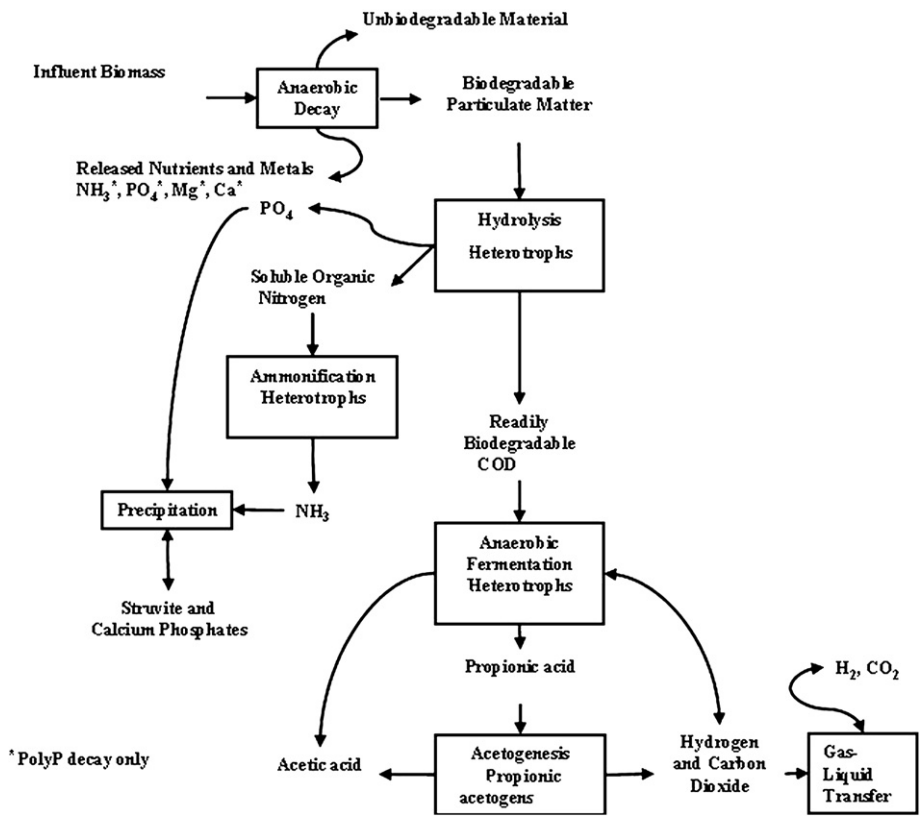

Fig. 2 – Conceptual schematic for the anaerobic degradation model in BioWin (Adapted from BioWin manual).

methanogens due to heat pre-treatment of the seed sludge, the methanogens growth was switched off in all modeling runs. A conceptual schematic of the biohydrogen production model is shown in Fig. 2. The following points pertaining to the fate of organics in the system describe the key stages:

- Influent biomass undergoes anaerobic decay in the digester. The process rates and stoichiometry are the same as for anaerobic decay in the activated sludge process. The products of decay include unbiodegradable organic, nitrogen, and phosphorus components.
- Hydrolysis of particulate matter is mediated by the (non-polyP) heterotrophs. Particulate matter may be present in the influent, or may consist of products from biomass decay. The products of hydrolysis are phosphate (PO_4–P), soluble organic nitrogen, and readily biodegradable COD.
- Non-polyP heterotrophs ferment the complex readily biodegradable COD to acetic acid, propionic acid hydrogen, and carbon dioxide. There are two model processes for this reaction step. One is for low dissolved hydrogen concentrations while the other is for high dissolved hydrogen concentrations. The stoichiometry of each of these processes is to be calibrated to achieve the appropriate product mix. The calibration can be done by trial and error to achieve the best match between modeled and measured data.
- Propionic acid is converted into acetic acid by acetogenic bacteria. This process also produces hydrogen and is switched off at high levels of propionate. The propionate inhibition constant is 10,000 mgCOD/L.

Table 2 – Wastewater fractions.

Name	Value
Readily biodegradable [gCOD/g of total COD]	0.8
Acetate [gCOD/g of readily biodegradable COD]	0
Non-colloidal slowly biodegradable [gCOD/g of slowly degradable COD]	0.5
Unbiodegradable soluble [gCOD/g of total COD]	0.018
Unbiodegradable particulate [gCOD/g of total COD]	0.04
Ammonia [gNH3-N/gTKN]	0.5
Particulate organic nitrogen [gN/g Organic N]	0.25
Soluble unbiodegradable TKN [gN/gTKN]	0.02
N:COD ratio for unbiodegradable part. COD [gN/gCOD]	0.035
Phosphate [gPO_4–P/gTP]	0.2
P:COD ratio for influent unbiodegradable part. COD [gP/gCOD]	0.011
Non-polyP heterotrophs [gCOD/g of total COD]	1.00E-04
Anoxic methanol utilizers [gCOD/g of total COD]	1.00E-04
Ammonia oxidizers [gCOD/g of total COD]	1.00E-04
Nitrite oxidizers [gCOD/g of total COD]	1.00E-04
Anaerobic ammonia oxidizers [gCOD/g of total COD]	1.00E-04
PAOs [gCOD/g of total COD]	1.00E-04
Propionic acetogens [gCOD/g of total COD]	1.00E-04
Acetoclastic methanogens [gCOD/g of total COD]	1.00E-04
H_2-utilizing methanogens [gCOD/g of total COD]	1.00E-04

Table 3 – Kinetic parameters for heterotrophs.

Name	Default	Value	Arrhenius
Max. spec. growth rate [1/d]	3.2	3.2	1.029
Substrate half sat. [mgCOD/L]	5	5	1
Aerobic decay [1/d]	0.62	0.62	1.029
anaerobic decay [1/d]	0.3	0.3	1.029
Anaerobic hydrolysis factor [–]	0.5	0.5	1
Adsorption rate of colloids [L/(mgCOD d)]	0.8	0.8	1.029
Fermentation rate [1/d]	3.2	3.2	1.029
Fermentation half sat. [mgCOD/L]	5	5	1
Hydrolysis half sat. [mgCOD/L]	0.15	0.15	1

The influent characteristics of the synthetic wastewater containing glucose used in the experimental study was simulated in the model using the influent specifier associated with BioWin model and revealed the fractions summarized in Table 2. As depicted in Table 3, the main kinetic parameters for heterotrophs (hydrogen producers) used in all modeling runs were set to default values.

3. Results and discussion

3.1. *Steady-state modeling*

Table 4 summarizes the main experimental results under six different organic loading rates, while complete experimental results are reported elsewhere [3]. The model was first calibrated using two sets of experimental data, namely OLR-1 and OLR-2. The calibration involved 180 runs where in tweaking the stoichiometry of the process by trial and error as mentioned earlier was completed to achieve the best fit of the experimental data. It was then validated using the remaining four sets of experimental data (i.e. OLR-3 to OLR-6). Figs. 3–5 show the correlation between various predicted and measured parameters for the 6 steady-state OLRs. The main parameters considered in the comparison were the biomass concentration in the hydrogen reactor measured as volatile suspended solids ($VSS_{reactor}$), biomass concentration in the clarifier supernatant (VSS_{eff}), solids retention time (SRT), main soluble metabolites (i.e. acetate, butyrate vs. propionate), volatile fatty acids (VFAs), soluble chemical oxygen demand in the effluent ($SCOD_{eff}$), hydrogen production rate, hydrogen production yield, and hydrogen content in the biogas.

Biomass concentration in hydrogen reactors is a key parameter for the stability and hydrogen production through the process as it directly affects the food-to-microorganisms (F/M) ratio [3]. In the literature, biohydrogen system failures were frequently attributed to marked decrease in biomass content in the hydrogen reactor due to severe cell washout [12,23,24]. Fig. 3a and b shows the correlation between predicted and measured biomass concentrations in both the hydrogen reactor and clarifier effluent for the six experimental runs. As apparent from Fig. 3a, the model accurately predicted reactor biomass concentrations throughout the observed range of 1400–18000 mgVSS/L at OLRs in the range of 6.5–206 gCOD/L-d, with an average percentage error (APE) of 4.6%. The APE is defined as the summation of the absolute difference between the experimental and predicted values divided by the experimental values, averaged over the number of data points. Similarly, the model predictions closely matched the observed biomass concentrations in the clarifier supernatant increase in the range of 200 mgVSS/L to around 6300 mgVSS/L over the same aforementioned range of OLR with an APE of 10% (see Fig. 3b). The successful model prediction of the biomass concentrations in both the hydrogen reactor and clarifier effluent was a result of the accurate modeling of the clarifier. As depicted in Fig. 3c, the model predicted the solids retention time well for the six experimental runs with an APE of 6.5%.

During the conversion of glucose to hydrogen a mixture of soluble metabolites (i.e. volatile fatty acids) are produced. The two main pathways for glucose conversion are the acetate and butyrate pathways can be given by:

$$C_6H_{12}O_6 + 2H_2O \rightarrow 2CH_3COOH + 2CO_2 + 4H_2 \quad (1)$$

$$C_6H_{12}O_6 \rightarrow CH_3CH_2CH_2COOH + 2CO_2 + 2H_2 \quad (2)$$

Considering Eqs. (1) and (2), the stoichiometric hydrogen yield would be 4 and 2 mol H_2/mol glucose, respectively. Although BioWin uses an alternative pathway to the butyrate pathway (i.e. glucose → propionate → acetate + hydrogen) (see Fig. 2), the predicted and measured acetate and butyrate concentrations agreed well for all experimental runs as can be noted from Fig. 4a and b, with APEs of 12% and 14.8%, respectively. These results were confirmed by the correlations shown in Fig. 4c and d for the total VFAs and the final SCOD with APE of 14% and 13%, respectively.

Table 4 – Summary of experimental results.

Measured parameters	OLR-1	OLR-2	OLR-3	OLR-4	OLR-5	OLR-6
VSS reactor (mg/L)	1489 ± 116	4190 ± 308	8915 ± 972	15703 ± 926	18472 ± 1404	17038 ± 883
VSS out (mg/L)	247 ± 46	744 ± 50	1578 ± 141	3073 ± 397	5565 ± 581	5240 ± 372
SCOD out (mg/L)	1492 ± 79	6023 ± 194	11922 ± 1230	21267 ± 1627	40960 ± 1624	59091 ± 1358
VFAs (mgCOD/L)	1491 ± 87	5924 ± 257	10344 ± 1114	17976 ± 1444	19232 ± 1156	20582 ± 1686
Hydrogen Gas (%)	71 ± 0.9	73 ± 2.7	65 ± 3.3	67 ± 2.7	43 ± 2.8	39 ± 1.5
Hydrogen Gas (L/d)	12 ± 1.3	48.1 ± 4.7	97 ± 5	179 ± 12	67 ± 5	60 ± 3.4
Yield (mol/mol)	2.8 ± 0.3	2.8 ± 0.3	2.9 ± 0.1	2.8 ± 0.3	1.2 ± 0.1	1.1 ± 0.1

Note. Values represent average ± standard deviation.

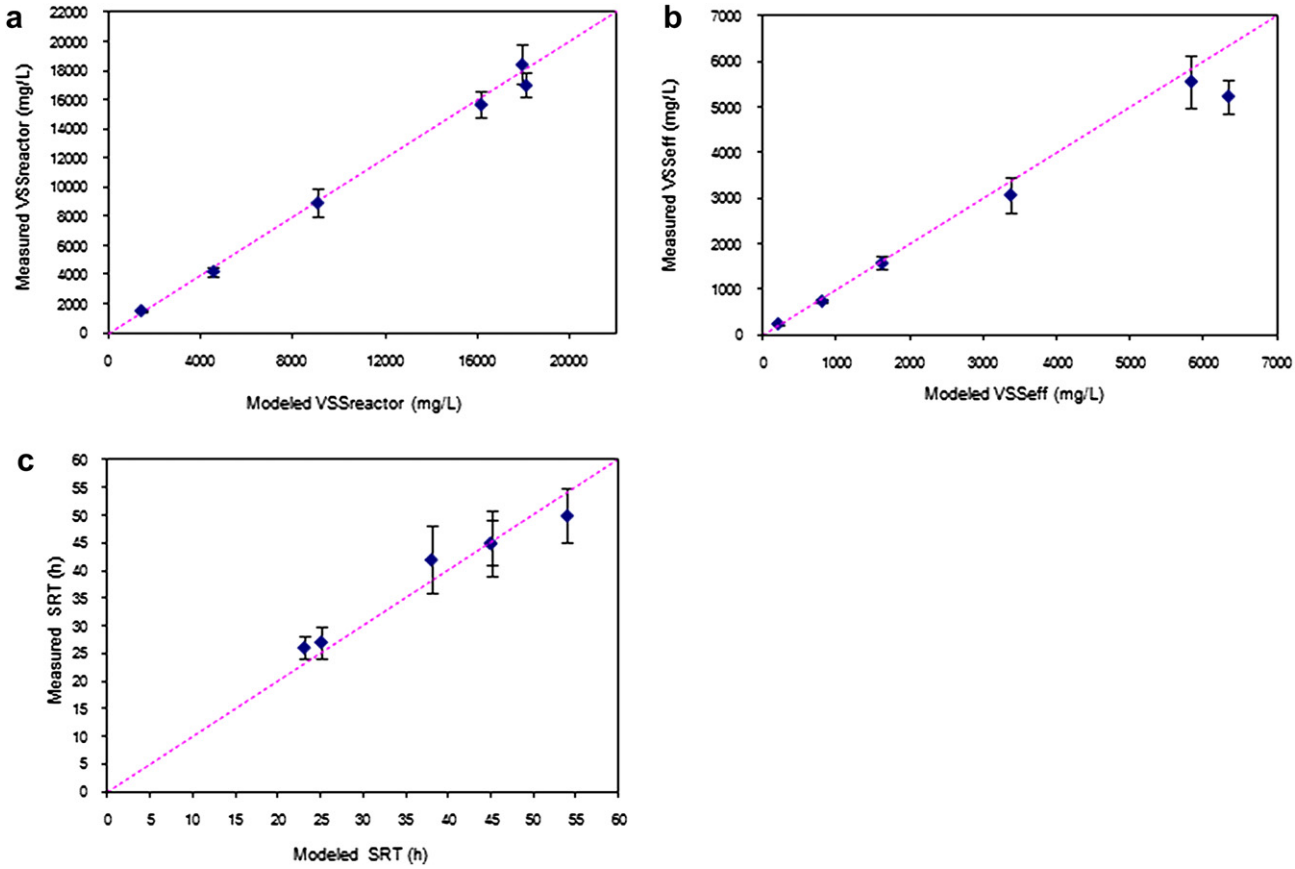

Fig. 3 – Correlation between modeled and measured parameters for: (a) reactor VSS, (b) effluent VSS, (c) SRT (Note: error bars represent standard deviations for experimental results).

As apparent from Fig. 5, the model accurately predicted both hydrogen production rate and hydrogen yield with a relatively low APE of 4%, while an error of less than 10% was observed when predicting the hydrogen content in the biogas. It is noteworthy that the reactor final pH from both experimental runs and the model was 5.5. Fig. 6 shows the relationship between hydrogen production rate and hydrogen yield at different OLRs from both measured and predicted data. As evident from Fig. 6, the model confirmed the linear increase in hydrogen production rate with the increase of the OLR up to 103 gCOD/L-d. On the other hand, the model predicted an almost constant hydrogen yield of 2.9–3.0 mol H_2/mol glucose during the same range of OLRs. The steady-state model solutions for OLR-5 and OLR-6 have revealed a decrease in hydrogen production rate and hydrogen yield to approximately 65 L/d and 1.2 mol H_2/mol glucose, respectively.

The high hydrogen yields achieved in the experimental study and corroborated by the model predictions were confirmed by the high biomass concentrations maintained in the hydrogen reactor as well as the operational *F/M* ratios that fell in the recommended range of 4.4–6.4 gCOD/gVSS-d reported in the literature. The authors' earlier work [3], using the experimental data reported here as well as additional data obtained from two CSTRs operated at OLRs of 25.7 and 42.8 gCOD/L-d and HRTs of 8 h and 12 h [23], demonstrated an inverse relationship between the biomass and hydrogen yields (i.e. low hydrogen yields were associated with high biomass yields). On the other hand, the stoichiometric yield of 4 and 2 mol H_2/mol glucose from Eqs. (1) and (2) are calculated neglecting any biomass yield. Thus, considering the biomass yield would eventually decrease due to energy (COD) utilization for biomass synthesis. Considering COD mass balances, Eqs. (1) and (2) can be modified to calculate the practical ranges of hydrogen yields from glucose conversion to a mixture of acetate and butyrate (neglecting all other factors that might hinder the efficiency), i.e.

$$H_2 \text{ Yield (mol } H_2\text{/mol glucose)} = 4\,(1-Y_{biomass}) \quad (3)$$

$$H_2 \text{ Yield (mol } H_2\text{/mol glucose)} = 2\,(1-Y_{biomass}) \quad (4)$$

where $Y_{biomass}$ is the biomass observed yield in gCOD/gCOD.

Assuming a typical biomass yield of 0.15 gCOD/$gCOD_{converted}$ reported for hydrogen producers [25] and substituting in Eqs. (3) and (4), the practical hydrogen yield should be in the range of 1.7–3.4 mol H2/mol glucose, while using the widely reported biomass yield of 0.4 gCOD/$gCOD_{converted}$ in CSTRs [3,23], the practical hydrogen yield ranges from 1.2 to 2.4 mol H_2/mol glucose. Eqs. (3) and (4) clearly justify that in fact an inverse relationship between the biomass and hydrogen yields does exist. Furthermore, based on the values of biomass and hydrogen yields from both

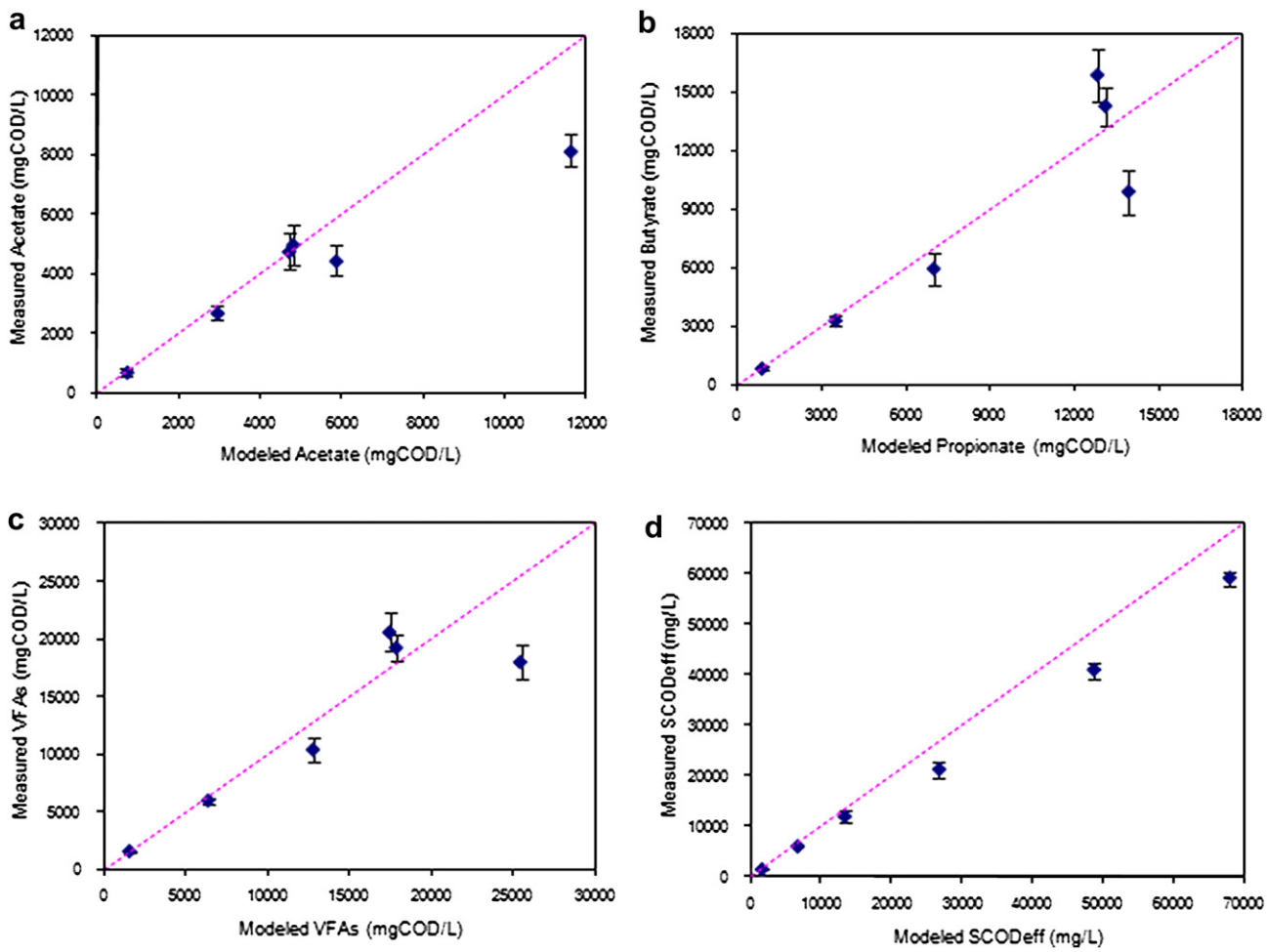

Fig. 4 – Correlation between modeled and measured parameters for: (a) acetate, (b) propionate vs. butyrate, (c) VFAs, (d) effluent SCOD (Note: error bars represent standard deviations for experimental results).

experimental and predicted results, the IBRCS achieved a maximum efficiency of 88% (a hydrogen yield of 3.0 mol H_2/mol glucose compared to a maximum practical H_2 yield of 3.4 mol H_2/mol glucose).

3.2. *Evaluation of decoupling of SRT from HRT*

After successful model calibration and verification, the clarifier was removed from the IBRCS to assess the performance of CSTR in comparison to the IBRCS at 4 different glucose concentrations (2 g/L, 8 g/L, 16 g/L and 32 g/L) corresponding to the optimal OLR-1 to OLR-4 (6.5–103 gCOD/L-d). The performance of the CSTR was strongly affected due to biomass washout. Fig. 7 compares the IBRCS and CSTR in terms of reactor VSS, hydrogen yield, hydrogen production rate, and total VFAs. The steady-state bioreactor VSS concentration in the CSTR dropped drastically to 120, 500, 1240 and 1970 mgVSS/L for the OLRs, as compared to 1400, 4550, 9000 and 16,100 mgVSS/L in the IBRCS. The extremely high *F/M* ratios of greater than 40 in the CSTR resulted in a low hydrogen yields ranging from 0.6 to 1.2 mol H_2/mol glucose. The maximum hydrogen production rate in the CSTR was approximately 53 L/d compared to a maximum of 194 L/d in the IBRCS and they were both achieved at an OLR of 103 gCOD/L-d. The total volatile fatty acids produced in the IBRCS at the 4 different OLRs were at least 3-fold higher than those produced in the CSTR. Thus, the BioWin model emphatically established the superior performance of the novel patent-pending IBRCS relative to the CSTR confirming the experimental observations widely reported in the literature [26–32].

3.3. *Impact of HRT reduction*

To study the impact of HRT reduction on the performance of the IBRCS, three steady-state simulation runs at HRT of 4 h, 2 h and 1 h utilizing 32 g/L of glucose were performed in comparison with the steady-state data from OLR-4 at 8 h HRT. As depicted in Fig. 8, hydrogen production rate decreased by 3%, 13% and 28% with the decrease in HRT from 8 h to 4 h, 2 h and 1 h, respectively. Even though hydrogen production rates seem to be slightly affected by the reduction in HRT, the hydrogen yields were drastically impacted. The hydrogen yield decreased drastically from 3 mol H_2/mol glucose at an HRT of 8 h–0.3 mol H_2/mol glucose at HRT of 1 h. It is noteworthy that the *F/M* ratio increased from 6.4 gCOD/gVSS-d at

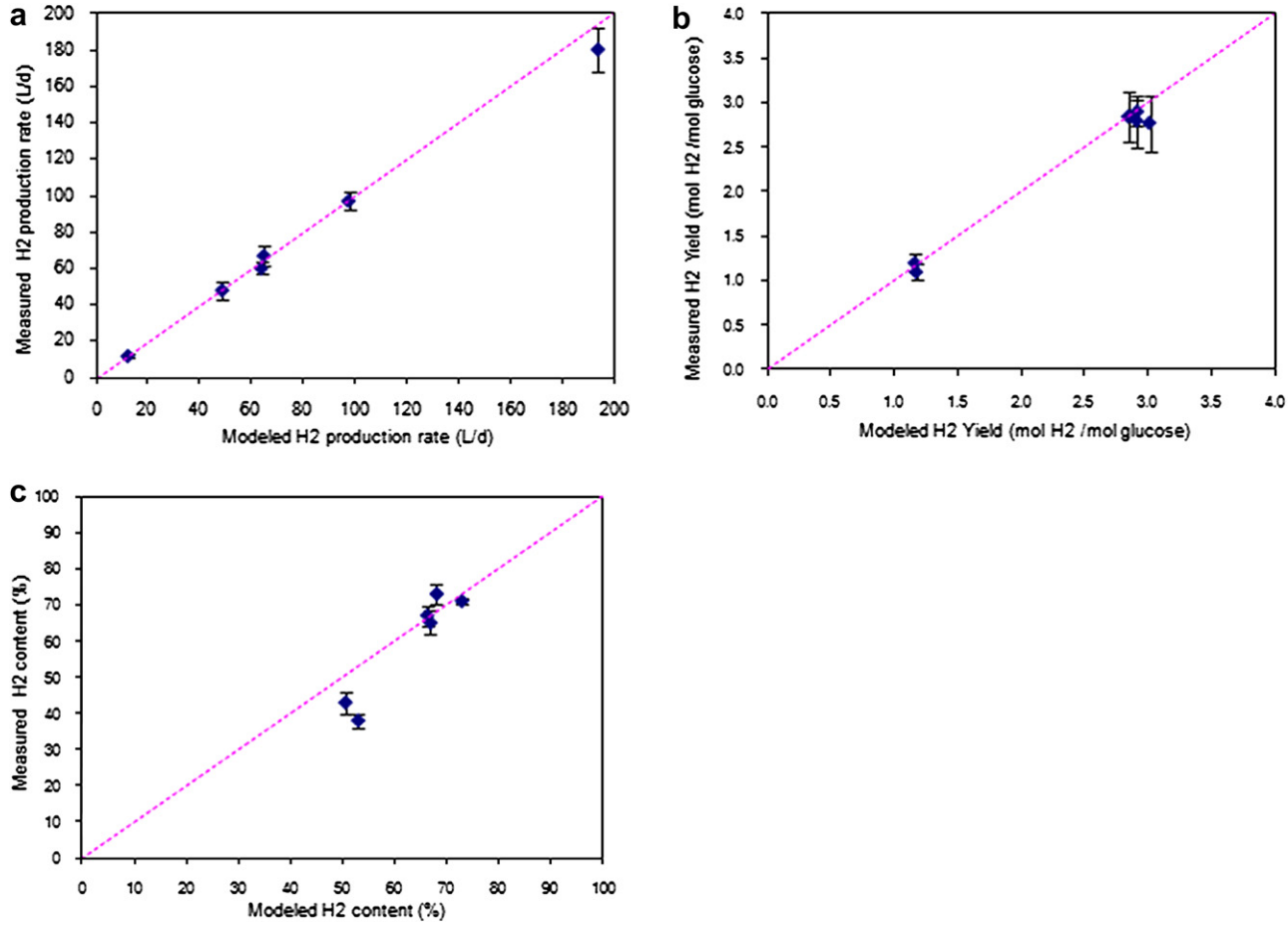

Fig. 5 – Correlation between modeled and measured parameters for: (a) H_2 production rate, (b) H_2 yield, (c) H_2 content (Note: error bars represent standard deviations for experimental results).

HRT of 8 h–12.8, 26 and 55 gCOD/gVSS-d at HRT of 4 h, 2 h and 1 h, respectively. The increase in *F/M* ratio was a result of a decrease in the solids retention time due to the increase of solids loading rate to the clarifier which was not sized up accordingly. Thus, it is postulated that sustained higher reactor biomass concentrations with proper clarification would have inevitably improved both hydrogen production rate and hydrogen yield.

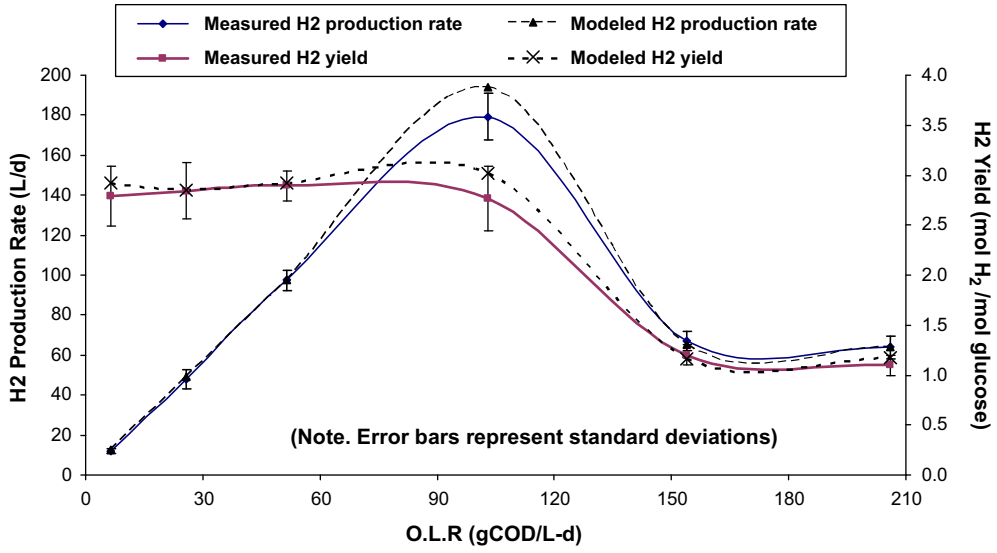

Fig. 6 – Relationship between hydrogen production rate and hydrogen yield vs. OLR.

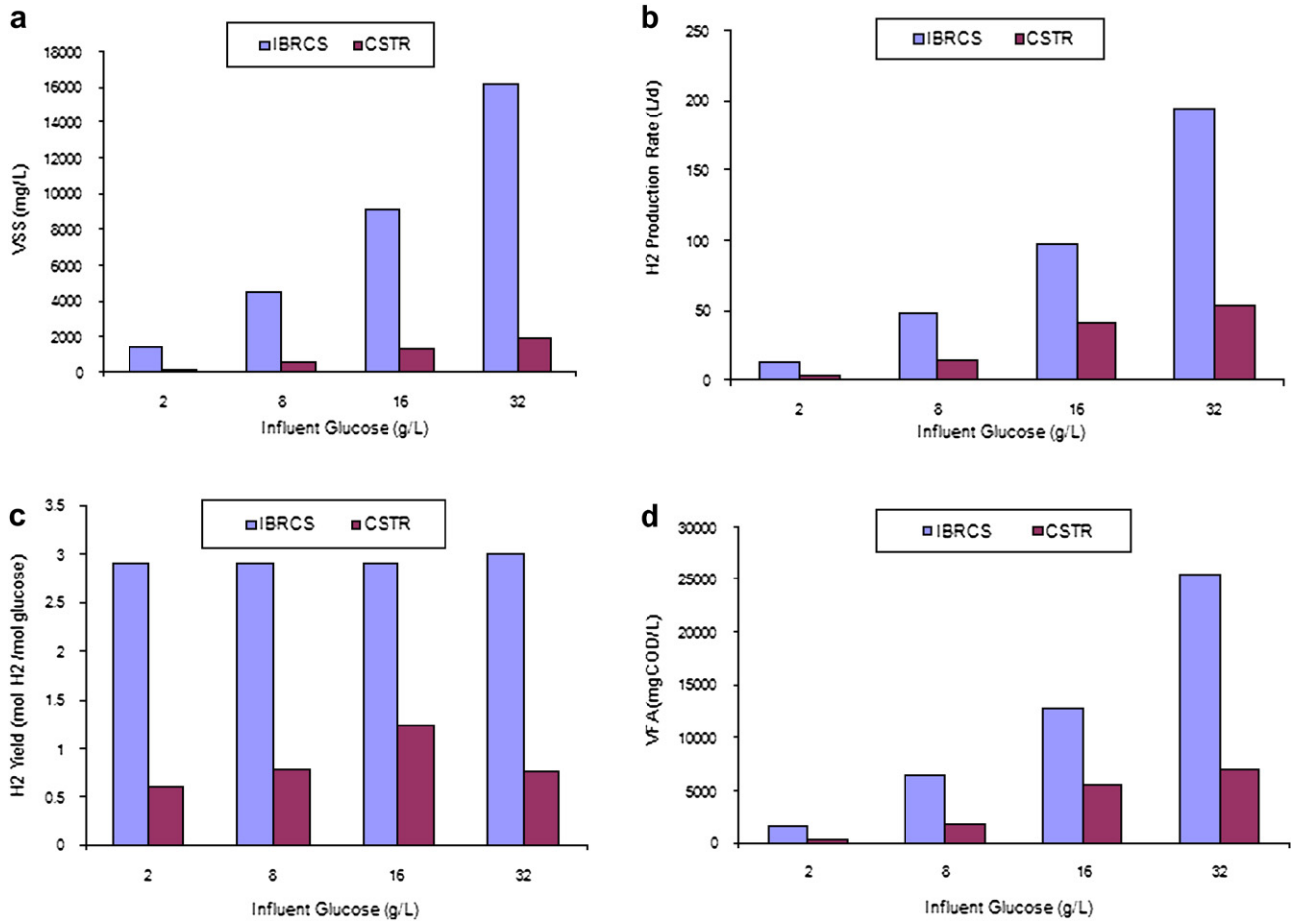

Fig. 7 – Comparison between the IBRCS and CSTR for: (a) reactor VSS, (b) H_2 production rate, (c) H_2 yield, (d) VFAs.

3.4. *Dynamic simulation of the IBRCS*

Dynamic simulation is an important tool to evaluate the performance of any biological system under variable harsh conditions that might occur in actual operational conditions. In biohydrogen production, this is considered the first study of the impact of dynamic short-term variable hydraulic and organic loading. It must be emphasized that the primary objective of the dynamic simulation was to test process performance primarily focusing on the bioreactor on the basis that clarification is not limiting. While this assumption may not be practically achievable in all applications, it was critical for the evaluation of the hydrogen bioreactor which has been shown to exhibit sensitivity to *F/M* ratios [3].

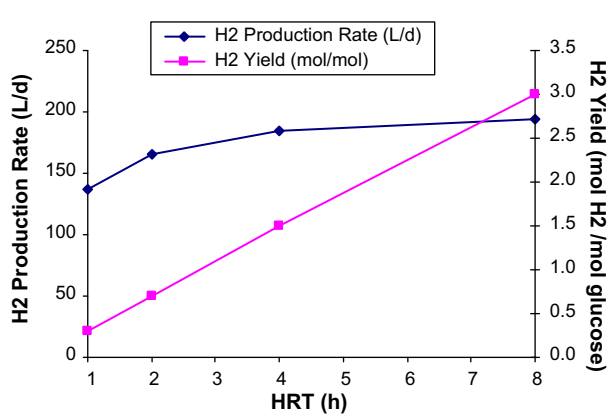

Fig. 8 – Relationship between hydrogen production rate and hydrogen yield vs. HRT.

3.4.1. *Short-term hydraulic loading*

To study the impact of short-term hydraulic loadings, the system was allowed to run for 22 days at SRT of 50 h. Five days were run at an HRT of 8 h with influent flow rate of 15 L/d and utilizing 32 g/L of glucose, the influent flow rate was then increased from 15 L/d to 120 L/d over five 2-day intervals, and was then reduced down to 15 L/d and kept running for 7 days. As depicted in Fig. 9a, the hydrogen production rate increased gradually over a period of 2.5 days to a maximum of 240 L/d and stabilized at approximately 195 L/d equivalent to a hydrogen yield of 3.1 mol H_2/mol glucose. The decrease of HRT from 8 h to 4 h resulted in an increase in the hydrogen production rate to 340 L/d (2.9 mol H_2/mol glucose), while at an HRT of 2 h the hydrogen production rate increased slightly to reach 380 L/d (1.6 mol H_2/mol glucose). With further reduction in HRT to 1 h, the hydrogen production rate dropped precipitously to 180 L/d (0.4 mol H_2/mol glucose). Over a period of 4 days, the system HRT was increased to reach its original

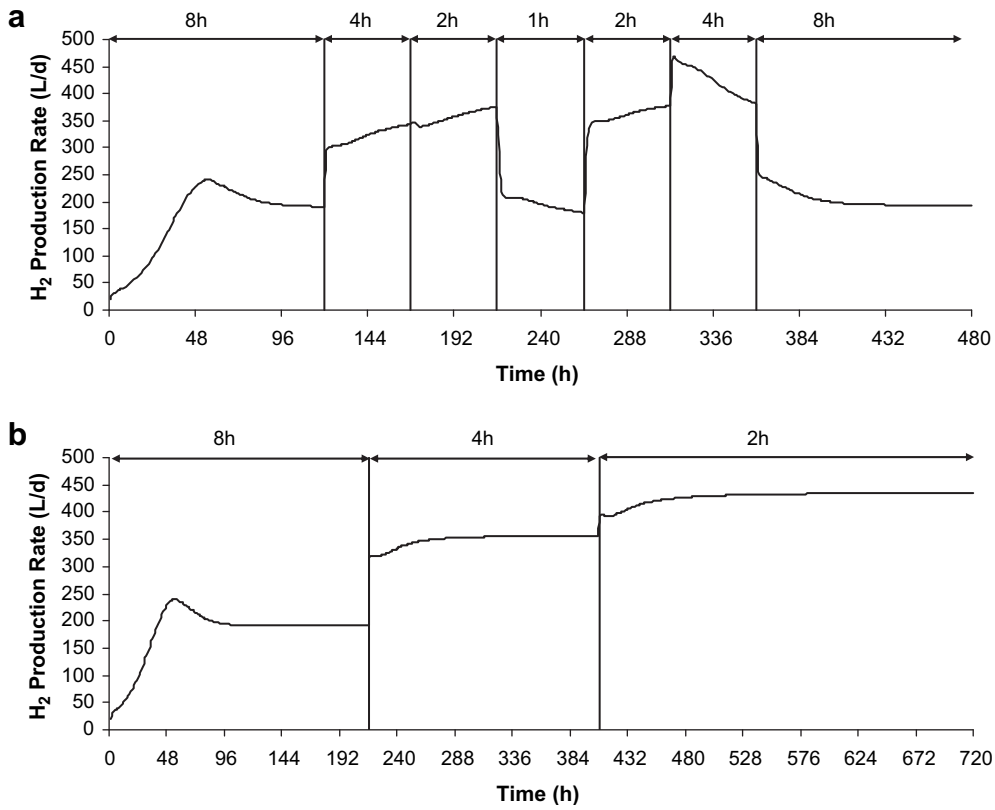

Fig. 9 – Diurnal variations in hydrogen production rate for: (a) short-term hydraulic loading, (b) long-term hydraulic loading.

operational HRT (8 h), where the original hydrogen production rate of 195 L/d was recovered.

3.4.2. *Long-term hydraulic loading*

Fig. 9b shows the diurnal performance of the system under an extended 30 days of operation at HRTs of 8 h, 4 h and 2 h sustained for 9 days, 8 days and 13 days, respectively. The relationship between hydrogen production rate and hydrogen yield at the three different HRTs is shown in Fig. 10. As evident from both figures, the hydrogen production rate increased from approximately 200 L/d to 440 L/d with the decrease in HRT from 8 h to 2 h, respectively. In addition, hydrogen yield was constant at 3.1 mol H_2/mol glucose at HRTs of 8 h and 4 h, and decreased to around 1.9 mol H_2/mol glucose at an HRT of 2 h.

3.4.3. *Short- and long-term organic loading*

Using the 4 optimum OLR (1–4) that showed a constant hydrogen yield of 2.9–3.0 mol H_2/mol glucose, a short-term dynamic simulation was performed (see Fig. 11a) at SRT of 50 h assuming that clarification is not limiting. After a 5-day startup period at OLR-1 (6.5 gCOD/L-d), the system was shock loaded over three 2-day intervals by OLR of 25.7 gCOD/L-d, 51.4 gCOD/L-d and 103 gCOD/L-d, denoted in Fig. 11 as OLR-2, OLR-3 and OLR-4, respectively. The OLR was then reduced gradually to 6.5 gCOD/L-d over two 2-day intervals at OLR-3 and OLR-2, simultaneously. Both hydrogen production rate and hydrogen yield followed the same pattern showed earlier in Fig. 6, i.e., the hydrogen production rate increased linearly with the increase in OLR to a maximum of 190 L/d and the hydrogen yield was constant at around 3.0 mol H_2/mol glucose.

Fig. 11b shows the diurnal dynamic simulation for hydrogen production rate over a period of 60 days under six OLRs ranging from 6.5 gCOD/L-d to 206 gCOD/L-d. The hydrogen production rate increased linearly from 12.8 L/d to 280 L/d with the increase in OLR from 6.5 gCOD/L-d to 154 gCOD/L-d, while the hydrogen yield was almost constant at 3.2 mol H_2/mol glucose (see Fig. 12). Further increase in OLR to 206 gCOD/L-d resulted in a marginal increase in the production rate to around 300 L/d corresponding to

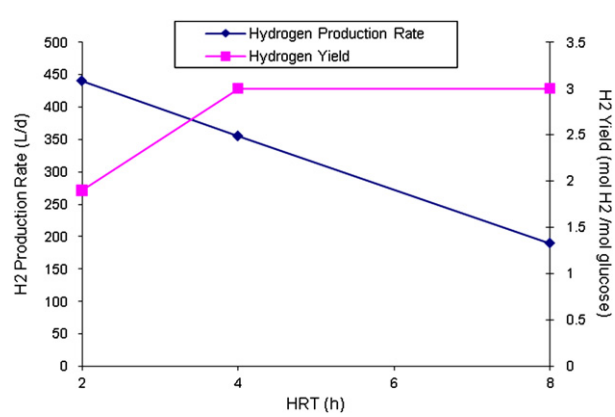

Fig. 10 – Relationship between hydrogen production rate and hydrogen yield from dynamic simulation vs. HRT.

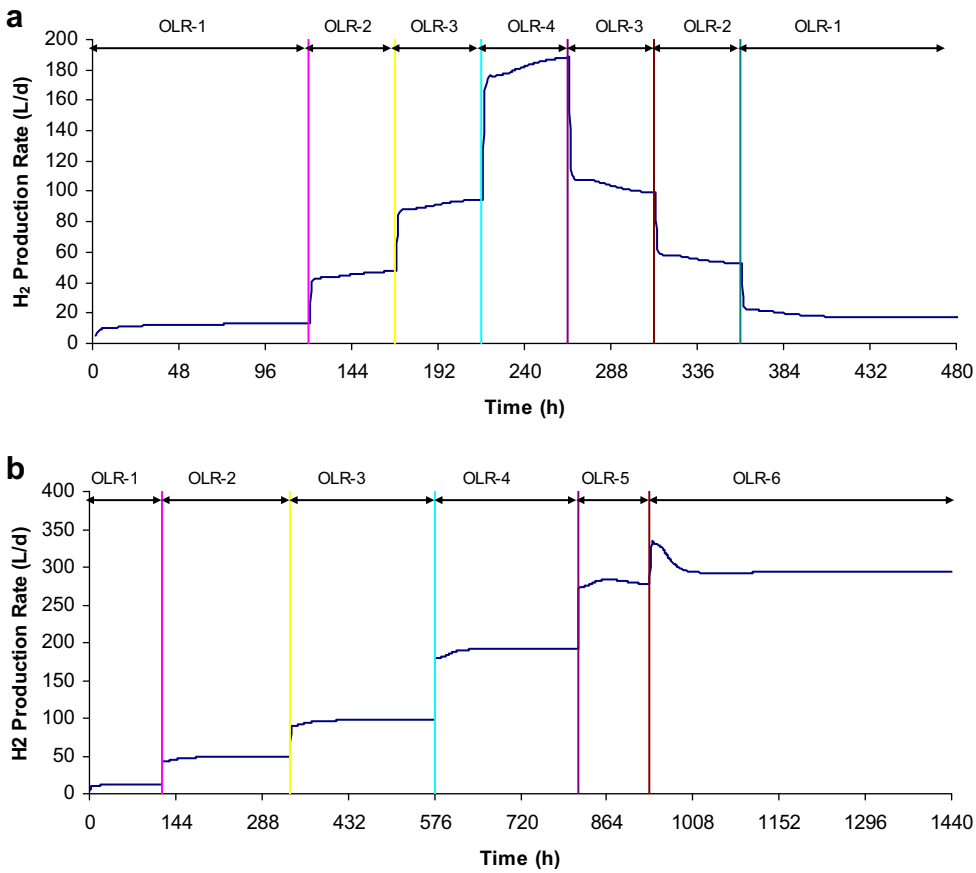

Fig. 11 – Diurnal variations in hydrogen production rate for: (a) short-term organic loading, (b) long-term organic loading.

a hydrogen yield of 2.5 mol H_2/mol glucose. The enhanced performance of the system at OLR-5 and OLR-6 during the long-term dynamic simulation compared to the modeled and experimental steady-state data showed in Fig. 6 reveals that the gradual increase in the OLR would be more beneficial than starting up the system at high OLR, i.e. step-wise increase in OLR to 206 gCOD/L-d could be sustained, thus emphasizing the importance of long startup times for high-rate biohydrogen systems.

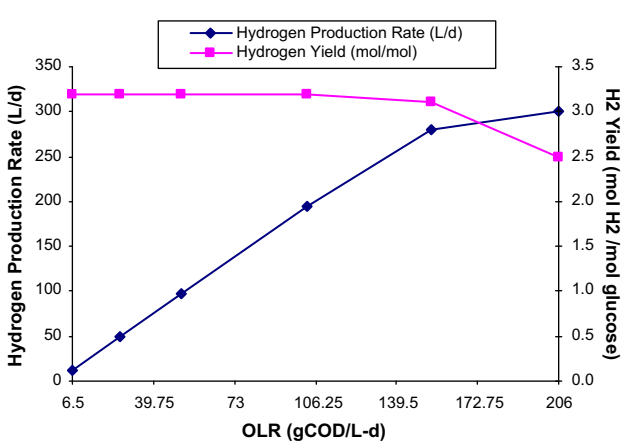

Fig. 12 – Relationship between hydrogen production rate and hydrogen yield from dynamic simulation vs. OLR.

4. Summary and conclusions

Both steady-state and dynamic modeling of biohydrogen production in the IBRCS using BioWin were evaluated in this study. The following conclusions can be drawn:

- The model accurately predicted biomass concentrations in both the bioreactor and the clarifier supernatant with average percentage errors (APEs) of 4.6% and 10%, respectively. Hydrogen production rates and hydrogen yields predicted by the model were in close agreement with the observed experimental results as reflected by an APE of less than 4%, while the hydrogen content was well correlated with an APE of 10%.
- Despite using a different pathway for biohydrogen production, the predicted and measured acetate and butyrate concentrations for the six experimental runs agreed well with APEs of 12% and 14.8%, respectively. These results were validated by the accurate prediction of total volatile fatty acids in the reactor with an APE of 14%.
- The calibrated model confirmed the advantages of decoupling of the solids retention time (SRT) from the hydraulic retention time (HRT) in biohydrogen production, with the average hydrogen yield decreasing from 3.0 mol H_2/mol glucose to 0.8 mol H_2/mol glucose upon elimination of the clarifier.

- Steady-state simulation for the IBRCS at HRT of 4 h, 2 h and 1 h utilizing 32 g/L of glucose showed that the hydrogen yield decreased drastically from 3.0 mol H_2/mol glucose at HRT of 8 h–1.5, 0.7 and 0.3 mol H_2/mol glucose for HRT of 4 h, 2 h and 1 h, respectively, due to washout as a result of clarifier limitation.
- Dynamic modeling showed that the system responds favorably to short-term hydraulic and organic surges, recovering back to the original condition. Furthermore, the dynamic simulation revealed that with a prolonged startup periods of 10 and 30 days and at SRT of 50 h, the IBRCS can be operated at an HRT of 4 h and OLR as high as 206 gCOD/L-d without substrate or product inhibition and/or marked performance deterioration, assuming that proper clarification is achievable.

REFERENCES

[1] Cheong DY, Hansen CL. Bacterial stress enrichment enhances anaerobic hydrogen production in cattle manure sludge. Appl Microbiol Biotechnol 2006;72:635–43.
[2] Wu KJ, Chang JS. Batch and continuous fermentative production of hydrogen with anaerobic sludge entrapped in a composite polymeric matrix. Proc Biochem 2007;42:279–84.
[3] Hafez H, Nakhla G, El Naggar H, Elbeshbishy E, Baghchehsaraee B. Effect of organic loading on a novel hydrogen bioreactor. Int J Hydrogen Energy 2010;35:81–92.
[4] Hafez H, Nakhla G, El Naggar H. Integrated system for hydrogen and methane production during landfill leachate treatment. Pending patent, US Patent Application US 61/202,137, 2009.
[5] Gadhamshetty V, Arudchelvam Y, Nirmalakhandan N, Johnson DC. Modeling dark fermentation for biohydrogen production: ADM1-based model vs. Gompertz model. Int J of Hydrogen Energy 2010;35:479–90.
[6] Jianlong W, Wei W. Kinetic models for fermentative hydrogen production: a review. Int J Hydrogen Energy 2009;34(8):3313–23.
[7] Chen X, Sun Y, Xiu Z, Li X, Zhang D. Stoichiometric analysis of biological hydrogen production by fermentative bacteria. Int J Hydrogen Energy 2006;31(4):539–49.
[8] Chen WH, Chen SY, Kumar KS, Sung S. Kinetic study of biological hydrogen production by anaerobic fermentation. Int J Hydrogen Energy 2006;31(15):2170–8.
[9] Mu Y, Yu HQ, Wang G. A kinetic approach to anaerobic hydrogen-producing process. Water Res 2007;41(5):1152–60.
[10] Zheng XJ, Yu HQ. Inhibitory effects of butyrate on biological hydrogen production with mixed anaerobic cultures. J Environ Manage 2005;74(1):65–70.
[11] Lin PY, Whang LM, Wu YR, Ren WJ, Hsiao CJ, Li SL, et al. Biological hydrogen production of the genus Clostridium: metabolic study and mathematical model simulation. Int J Hydrogen Energy 2007;32(12):1728–35.
[12] Whang LM, Hsiao CJ, Cheng SS. A dual-substrate steady-state model for biological hydrogen production in an anaerobic hydrogen fermentation process. Biotechnol Bioeng 2006;95(3):492–500.
[13] Andrews JF. Dynamic model of the anaerobic digestion process. J Sanit Eng Div Proc ASCE 1969;95:95–116.
[14] Andrews JF, Graef SP. Dynamic modeling and simulation of the anaerobic digestion process. In: Gould RF, editor. Anaerobic biological treatment processes. Advances in Chemistry series, 105. New York: American Chemical Society; 1971. p. 126–62.
[15] Hill DT, Barth CL. A dynamic model for simulation of animal waste digestion. J Wat Pollut Control Fed 1977;10:2129–43.
[16] Mosey FE. Mathematical modeling of the anaerobic digestion process: regulatory mechanisms for the formation of short chain volatile acids from glucose. Wat Sci Tech 1983;21:187–96.
[17] Costello DJ, Greenfield PF, Lee PL. Dynamic modeling of a single stage high rate anaerobic reactor – I. Model derivation. Wat Res 1991;25:847–58.
[18] Jones RM, MacGregor JF, Murphy KL, Hall ER. Towards a useful dynamic model of the anaerobic digestion process. Wat Sci Technol 1992;25(7):61–72.
[19] Batstone DJ, Keller J, Angelidaki I, Kalyuzhni SV, Pavlostathis SG, Rozzi A, et al. Anaerobic digestion model No. 1 (ADM1); 2002. Report No. 13.
[20] Peiris BRH, Rathnashri PG, Johansen JE, Kuhn, Bakke R. ADM1 simulations of hydrogen production. Water Sci Technol 2006;53(8):129–37.
[21] Rodriguez J, Kleerebezem R, Lema JM, van Loosdrecht MCM. Modeling product formation in anaerobic mixed culture fermentations. Biotechnol Bioeng 2006;93(3):592–606.
[22] Rodriguez J, Lema JM, van Loosdrecht MCM, Kleerebezem R. Variable stoichiometry with thermodynamic control in ADM1. Water Sci Technol 2006;54(4):101–10.
[23] Hafez H, Baghchehsaraee B, Nakhla G, Karamanev D, Margaritis A, El Naggar MH. Comparative assessment of decoupling of biomass and hydraulic retention times in hydrogen production bioreactors. Int J Hydrogen Energy 2009;34:7603–11.
[24] Wu SY, Hung CH, Lin CY, Lin PJ, Lee KS, Lin CN, et al. HRT-dependent hydrogen production and bacterial community structure of mixed anaerobic microflora in suspended, granular and immobilized sludge systems using glucose as the carbon substrate. Int J Hydrogen Energy 2008;33(5):1542–9.
[25] Chen CC, Lin CY, Chang JS. Kinetics of hydrogen production with continuous anaerobic cultures utilizing sucrose as the limiting substrate. Appl Microbiol Biotechnol 2001;57(1–2):56–64.
[26] Zhang JJ, Li XY, Oh SE, Logan BE. Physical and hydrodynamic properties of flocs produced during biological hydrogen production. Biotechnol Bioeng 2004;88(7):854–60.
[27] Oh SE, Lyer P, Bruns MA, Logan BE. Biological hydrogen production using a membrane bioreactor. Biotechnol Bioeng 2004;87(1):119–27.
[28] Kyazze G, Martinez-Perez N, Dinsdale R, Premier GC, Hawkes FR, Guwy AJ, et al. Influence of substrate concentration on the stability and yield of continuous biohydrogen production. Biotechnol Bioeng 2006;93(5):971–9.
[29] Lin CY, Jo CH. Hydrogen production from sucrose using an anaerobic sequencing batch reactor process. J Chem Technol Biotechnol 2003;78(6):678–84.
[30] Fang HHP, Liu H, Zhang T. Characterization of a hydrogen-producing granular sludge. Biotechnol Bioeng 2002;78(1):44–52.
[31] Van Ginkel SW, Logan B. Increased biological hydrogen production with reduced organic loading. Water Res 2005;39(16):3819–26.
[32] Wu SY, Hung CH, Lin CN, Chen HW, Lee AS, Chang JS. Fermentative hydrogen production and bacterial community structure in high-rate anaerobic bioreactors containing silicone-immobilized and self-flocculated sludge. Biotechnol Bioeng 2006;93(5):934–46.